ORIGINAL ARTICLE

Finite element analysis of FRP-strengthened RC beams

Teeraphot Supaviriyakit[1], Phuwanat Pornpongsaroj[1] and Amorn Pimanmas[2]

Abstract

Supaviriyakit, T., Pornpongsaroj, P. and Pimanmas, A.
Finite element analysis of FRP-strengthened RC beams
Songklanakarin J. Sci. Technol., 2004, 26(4) : 497-507

This paper presents a non-linear finite element analysis of reinforced concrete beam strengthened with externally bonded FRP plates. The finite element modeling of FRP-strengthened beams is demonstrated. Concrete and reinforcing bars are modeled together as 8-node isoparametric 2D RC element. The FRP plate is modeled as 8-node isoparametric 2D elastic element. The glue is modeled as perfect compatibility by directly connecting the nodes of FRP with those of concrete since there is no failure at the glue layer. The key to the analysis is the correct material models of concrete, steel and FRP. Cracks and steel bars are modeled as smeared over the entire element. Stress-strain properties of cracked concrete consist of tensile stress model normal to crack, compressive stress model parallel to crack and shear stress model tangential to crack. Stress-strain property of reinforcement is assumed to be elastic-hardening to account for the bond between concrete and steel bars. FRP is modeled as elastic-brittle material. From the analysis, it is found that FEM can predict the load-displacement relation, ultimate load and failure mode of the beam correctly. It can also capture the cracking process for both shear-flexural peeling and end peeling modes similar to the experiment.

Key words : FRP, strengthening, FEM, nonlinear analysis, peeling failure

[1]Graduate Student in Civil Engineering [2]Ph.D.(Structural Engineering), Asst. Prof., Sirindhorn International Institute of Technology, Thammasat University, Rangsit Center, Khlong Luang, Pathum Thani, 12121 Thailand.
Corresponding e-mail: amorn@siit.tu.ac.th
Received, 9 December 2003 Accepted, 2 February 2004

บทคัดย่อ

ธีระพจน์ ศุภวิริยะกิจ ภูวณัฐ พรพงษาโรจน์ และ อมร พิมานมาศ

การวิเคราะห์กำลังรับน้ำหนักของคานเสริมกำลังด้วยแผ่นไฟเบอร์อิลีเมนต์แบบไม่เชิงเส้น

ว. สงขลานครินทร์ วทท. 2547 26(4) : 497-507

บทความนี้นำเสนองานวิจัยเรื่องของการวิเคราะห์กำลังรับน้ำหนักและลักษณะการวิบัติของคานค.ส.ล.ที่เสริมกำลังด้วยแผ่นไฟเบอร์ (FRP) โดยวิธีไฟไนต์อิลีเมนต์แบบไม่เชิงเส้น ในวิธีไฟไนต์อิลีเมนต์ คอนกรีตและเหล็กเสริมถูกจำลองโดยใช้อิลีเมนต์คอนกรีตเสริมเหล็กไอโซพาราเมตริกชนิด 8 โนด สำหรับแผ่น FRP ที่ใช้ในการเสริมกำลังจะจำลองโดยใช้อิลีเมนต์อีลาสติกไอโซพาราเมตริกชนิด 8 โนด ส่วนกาวอีพอกซีที่ใช้ในการติดแผ่น FRP เข้ากับคานจำลองโดยการยึดโนดของคอนกรีตกับโนดของแผ่น FRP โดยตรง เนื่องจากไม่พบการวิบัติที่รอยต่อบริเวณกาวอีพอกซี จึงถือได้ว่ากาวอีพอกซียึดติดกับคานตลอดการรับน้ำหนักบรรทุก ความถูกต้องของการวิเคราะห์ด้วยวิธีไฟไนต์อิลีเมนต์นั้น ขึ้นอยู่กับแบบจำลองความเค้น-ความเครียดของคอนกรีต เหล็กเสริม และแผ่น FRP รอยร้าวและเหล็กเสริมในคอนกรีตจะจำลองในลักษณะกระจายไปทั่วอิลีเมนต์ (smeared) แบบจำลองความเค้น-ความเครียดของคอนกรีตประกอบด้วยแบบจำลองรับแรงดึงตั้งฉากกับรอยร้าว แบบจำลองรับแรงอัดขนานกับรอยร้าว และแบบจำลองรับแรงเฉือนขนานกับรอยร้าว แบบจำลองความเค้น-ความเครียดของเหล็กคำนึงถึงพฤติกรรมครากและแรงยึดเหนี่ยวระหว่างคอนกรีตและเหล็กเสริม ส่วนแบบจำลองความเค้น-ความเครียดของแผ่น FRP กำหนดให้แสดงพฤติกรรมอีลาสติกแบบเปราะ ผลการวิเคราะห์ พบว่าวิธีไฟไนต์อิลีเมนต์สามารถทำนายความสัมพันธ์ระหว่างน้ำหนักบรรทุกและการเคลื่อนตัว น้ำหนักบรรทุกสูงสุด และลักษณะการวิบัติของคานได้อย่างถูกต้องตรงกับผลการทดลอง และยังสามารถทำนายพฤติกรรมการหลุดลอกทั้งแบบการหลุดลอกที่ฐานรอยร้าวเอียง และการหลุดลอกที่ปลายแผ่น FRP ได้อย่างถูกต้อง

สาขาวิศวกรรมโยธาและระบบสิ่งก่อสร้าง สถาบันเทคโนโลยีนานาชาติสิรินธร มหาวิทยาลัยธรรมศาสตร์ ศูนย์รังสิต อำเภอคลองหลวง จังหวัดปทุมธานี 12121

The need to increase the capacity of the existing structures has recently become one of the most active areas in civil engineering. Several strengthening methods have been used in the past with varying degree of success. These include 1) enlargement of the cross section, 2) addition of new steel members, 3) steel plate bonding, 4) external post-tensioning, 5) reduction of span length, and recently 6) external bonding with FRP plate. FRP is a composite material consisting of numerous high-strength fibers impregnated in resin. It is gaining popularity for structural strengthening because of its high tensile strength, low weight and high durability (no corrosion) (Hollaway and Leeming,1999)

FRP has been successfully used to increase the flexural and shear capacities of RC beams (Saadatmanesh and Ehsani,1990). However, many experimental results have shown the premature failure due to peeling of FRP plate before the enhanced capacity is reached (Ritchie *et al*,1991). Arduini and Nanni (1997) described two common types of peeling failure, that is, end peeling and shear-flexural peeling as shown in Figure 1. The end peeling results from the combination of shear and normal tensile stress localized in the vicinity of the plate end. When the principal tensile stress reaches the tensile strength of concrete, a crack initiates and propagates horizontally at the level of tension steel, ripping off the concrete cover. The shear-flexural peeling initiates at the base of the flexural or shear-flexural crack, and propagates towards the support.

These failures are highly undesirable due to their brittleness. In order to ensure the safe design of structures, the load capacity associated with these failures must be accurately evaluated. However, presently there are no commonly acceptable

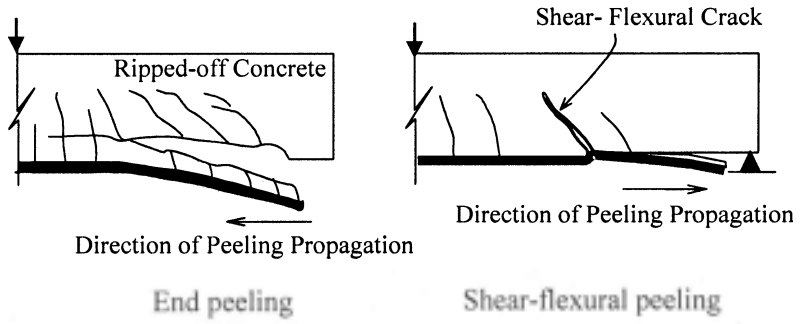

Figure 1. Typical peeling failures of FRP-strengthened beam.

design methods to predict the peeling failure load yet. In this paper, the authors employ the non-linear finite element method to predict the peeling failure load.

Significance of research

Currently, FRP materials have been widely used to increase the flexural and shear capacity of RC members. FRP plate is advantageous over steel plate due to its low weight, high strength and non-corrosive property. However, there is no standard reliable design method for preventing the peeling failure due to lack of sufficient experimental data. Since the peeling failure is very brittle, it is imperative to assess the load capacity associated with these failures accurately to ensure the structural safety for design. FEM analysis using non-linear constitute models of cracked concrete and reinforcing bars is proposed to predict the stress concentration at the plate end as well as at the base of diagonal cracks. This leads to the understanding in the failure mechanism, damage zone and load capacity.

Finite element modeling of FRP-strengthened beam

The typical finite element mesh of the FRP-strengthened beam is shown in Figure 2. The mesh consists of concrete, steel bars and FRP plates. The concrete and reinforcing steel are modeled together by 8-node 2-D isoparametric plane stress RC element. The RC element considers the effect of cracks and reinforcing steel as being smeared over the entire element.

Assuming perfect compatibility between reinforcing steel and cracked concrete, the 2-D stress vector of the entire element is the direct addition of concrete according to eq. (1).

$$\{\sigma\}_{rc} = \{\sigma\}_{c} + \{\sigma\}_{r} \quad (1)$$

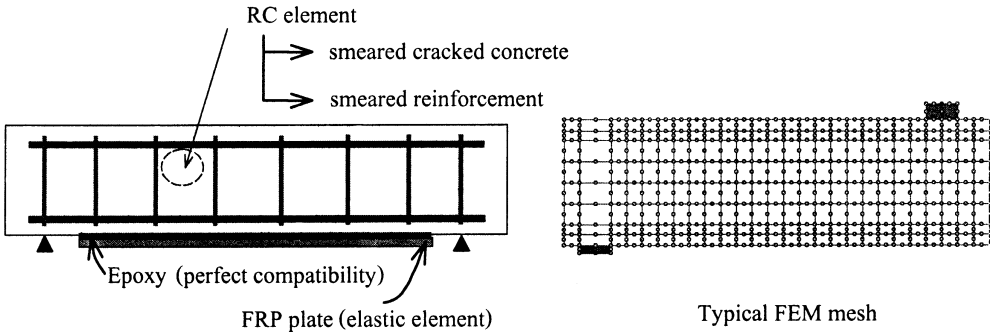

Figure 2. Finite element modeling and typical finite element mesh.

where $\{\sigma\}_{rc}$, $\{\sigma\}_c$ and $\{\sigma\}_r$ are stresses of reinforced concrete, cracked concrete and reinforcing bar, respectively.

Concrete cracks and reinforcing steel are treated in a smeared manner. The four-way fixed crack model developed by Okamura and Maekawa (1991) and Fukuura and Maekawa (1999) is used to deal with cracks in concrete. This four-way cracking model can deal with up to four cracks in arbitrary directions. As will be shown later, the rotation of a crack in any element hardly occurs due to the localized failure nature. Hence, the four-way fixed crack model is considered sufficient for the problem concerned.

The FRP plate is modeled by 2D elastic element. The epoxy layer can also be modeled by 2D elastic elements. However, the epoxy is usually much stronger than concrete and is therefore not a weak link in the FRP strengthened beam. As will be shown in the experiment, no failure takes place at the epoxy-bonding interface, so the full compatibility between FRP and beam soffit may be assumed. This is done by directly joining the node of FRP element with concrete element without using the elastic elements representing epoxy.

Local Constitutive Models of Cracked Concrete, Reinforcing Bars and FRP Plates

The local constitutive models of concrete (cracked and uncracked state), steel bars and FRP plates are essential to deal with concrete cracking, reinforcement yielding, crushing failure and elastic-brittle characteristics of FRP plate. The following sections explain the constitutive models of cracked concrete, reinforcing bars and FRP plate.

1. Cracked Concrete

The local strain vector (with respect to the crack axis) of cracked concrete consists of tensile strain normal to a crack, ε_n, compressive strain parallel to a crack, ε_t, and the shear strain along crack interface, γ_{cr} as shown in Figure 3. The constitutive laws can be defined as the uni-axial relations between the average stress and average strain as follows.

$$\sigma_n = \sigma(\varepsilon_n, \varepsilon_t, \eta_{1,2,\ldots,n}) \tag{2}$$

$$\sigma_t = \sigma(\varepsilon_t, \varepsilon_n, \eta_{n+1,\ldots,2n}) \tag{3}$$

$$\tau_c = \tau(\gamma_{cr}, \varepsilon_n, \varepsilon_t, \eta_{2n+1,\ldots}) \tag{4}$$

where σ_n, σ_t and τ_c represent the constitutive laws for computing normal tensile, compressive and shear stresses, respectively, η represents the set of path-dependent parameters. The formulation of the above constitutive laws and the path-dependent parameters were already reported (Maekawa *et al*, 2003). In the following, only the formula for envelope will be given.

The above constitutive laws correspond to three degrees of freedom of a cracked element,

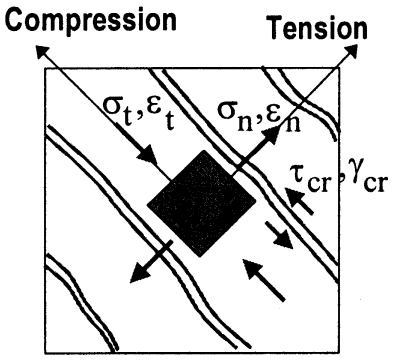

Figure 3. Degree of freedom for cracked concrete.

namely, tension stiffening/softening model normal to the crack, compression model parallel to the crack and shear transfer model along the crack interface. The coupling between shear and normal action is not explicitly considered in the formulation of stiffness matrix. The shear dilatancy is implicitly considered by adding the induced compressive normal stress due to shear to the computed normal stress orthogonal to the crack axis.

1.1 Coupled compression-tension model for normal stresses parallel and perpendicular to crack

The constitutive law for computing normal stresses (denoted by σ_n and σ_t in eq. (2) and (3) above) is the coupled compression-tension model as shown in Figure 4. For concrete in tension, the model covers both the softening due to aggregate bridging at the crack plane as well as the tension stiffening effect due to bond stress transfer between concrete and steel bar. For the envelope in tension, the model can be expressed as follows

$$\sigma_n = f_t \left(\frac{\varepsilon_{tu}}{\varepsilon_n} \right)^c \tag{5}$$

where σ_n is the tensile stress normal to crack, ε_{tu} is the cracking strain, c is softening/stiffening parameter. The parameter "c" indicates the rate of drop in tensile stress of concrete after cracking. It is set to be 0.4 for concrete element containing reinforcement and 2.0 for plain concrete element. The higher value of "c" indicates the more sudden decrease in concrete tensile stress after cracking. By using the appropriate value of "c" for each concrete element, the localized failure can be covered according to the fracture mechanics theory.

For compression parallel to the crack direction, the normal stress is computed using the elasto-plastic fracture model as follows

$$\sigma_t = K_0 E_{c0} (\varepsilon_t - \varepsilon_p) \tag{6}$$

Where σ_t is the compressive stress parallel to crack, K_0 is the fracture parameter representing the continuum damage as a result of dispersed cracking in concrete, E_{c0} is the initial stiffness and ε_p is the compressive plastic strain. The model combines the non-linearity of plasticity and fracturing damages to account for the permanent deformation and loss of elastic strain energy capacity, respectively. The reduced compressive stress due to transverse tensile strain is considered in the model as additional damage.

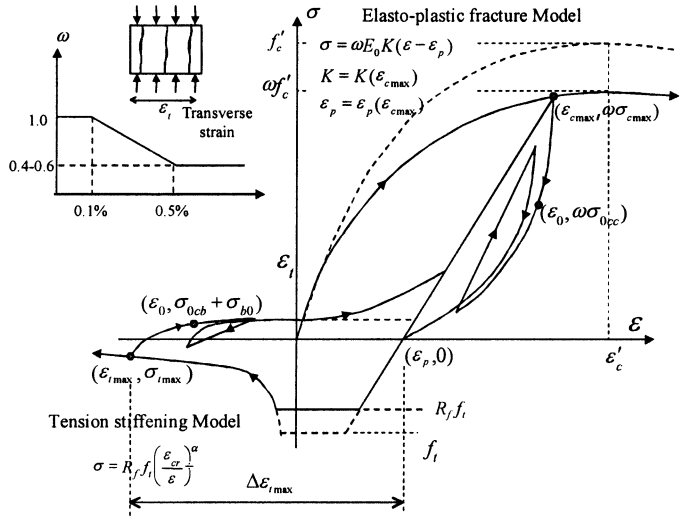

Figure 4. Coupled compression-tension model for normal stresses parallel and perpendicular to a crack.

1.2 Shear transfer model

For computing shear stress along the crack interface and the shear stiffness of the crack, the contact density model (Okamura and Maekawa, 1991; and Maekawa *et al*, 2003) is used for the envelope (Figure 5). The following equations give shear stress and shear stiffness along the crack,

$$\tau = f_{st}\frac{\beta^2}{1+\beta^2} \tag{7}$$

$$G_{cr} = \frac{\tau(\beta)}{\gamma_{cr}} \tag{8}$$

where f_{st} is shear strength transfer along the crack. β is the normalized shear strain defined as follows.

$$\beta = \frac{\gamma_{cr}}{\varepsilon_n} \tag{9}$$

For the cracked RC element, The imposed total shear strain (γ) compatible with the assumed nodal displacement can be separated into the shear strain due to un-cracked concrete part (γ_0) and shear strain due to cracks (γ_{cr}) as below

$$\gamma = \gamma_0 + \gamma_{cr} \cong \gamma_{cr} \tag{10}$$

Generally, shear strain due to un-cracked concrete part is relatively small compared with shear strain to crack, thus it can be ignored

2. Modeling of reinforcing bar

Local strain vector of reinforcing bar is defined along the bar axis. Reinforcing bar is modeled in the smeared concept, that is, it is assumed uniformly distributed over the whole element. This representation is adopted since it does not require additional nodes and elements. For reinforcing steel, compressive strains are usually smaller than tensile strains, thus reinforcement hardly yields in compression before spalling of concrete cover has occurred. At the tension side, however, the highly localized plasticity at the vicinity of cracks has to be taken into account. Due to bond effect, the average yield stress is lower than that of bare bar.

Thus the modeling of reinforcing bar in compression and tension can be different. For compression, the bilinear bare bar model is assumed in the analysis. For tension, the average stress-strain relationship considering the effect of bond between concrete and steel bar is adopted. Figure 6 shows stress-strain model of reinforcing bar. Since cracks in reinforced concrete element need not be orthogonal with the reinforcement direction, the bond effect may not be fully functional in such case. Reinforcing bar orthogonal to crack is supposed to have full bond effect. On the contrary, reinforcing bar parallel to crack is supposed to follow bare bar behavior. Therefore, the computation of mean yield strength has to take into account

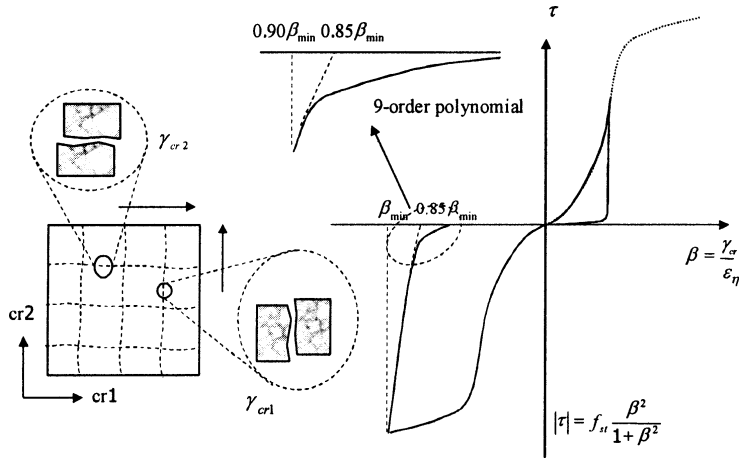

Figure 5. Shear transfer model.

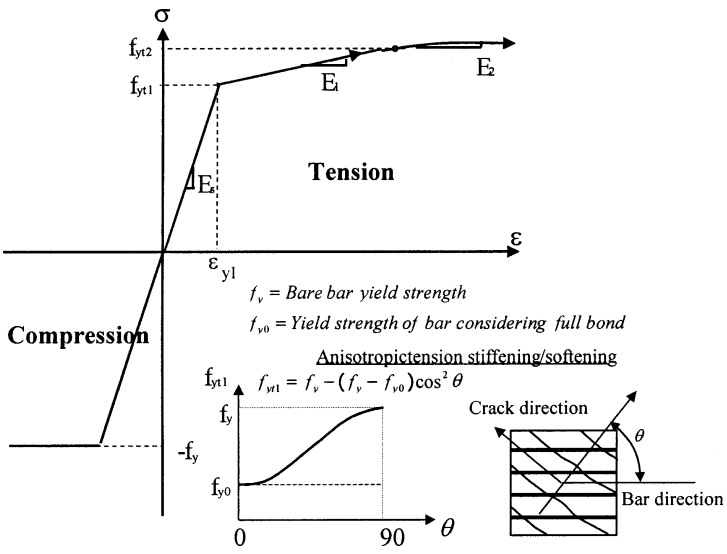

Figure 6. Reinforcing bar model.

the angular deviation of normal to crack from reinforcing bar direction (Maekawa *et al*, 2003).

3. Modeling of FRP plate

The FRP plate is modeled as elasto-brittle material. The stress-strain model is shown in Figure 7. The stress is linear up to the tensile strength and drops sharply to zero, representing the fracture of FRP plate.

Failure Criterion

In the finite element program, the failure is assumed to occur when one of the strain components ε_n, ε_t and γ_{cr} attains a certain value specified as limiting failure strain. For the RC element based on RC smeared crack model as shown in Figure 3, these failure strains are set as follows, (1) for tension failure, ε_n = 0.03, (2) for compression failure, ε_t = -0.01, and (3) for shear failure, γ_{cr} = ±0.02.

Numerical Verification

Recently, the authors have conducted the test on peeling characteristics of FRP-strengthened beams (Pornpongsaroj and Pimanmas, 2003). The objective of the test was to investigate the effect

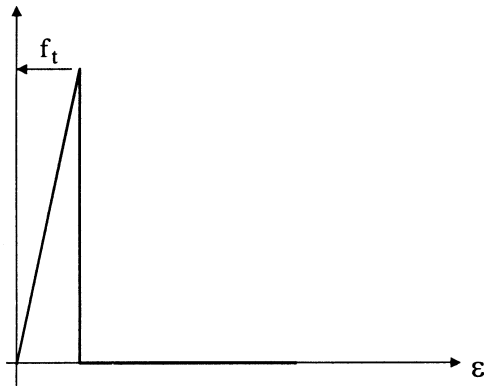

Figure 7. FRP stress-strain model.

Table 1. Material Properties (obtained from laboratory testing and used in finite element analysis)

Material	Yield Strength (MPa)	Ultimate Strength (MPa)	Elastic Modulus (MPa)
DB 16	532.98	606.94	2.0×10^5
DB 12	461.66	615.77	2.0×10^5
RB 6	383.77	493.05	2.0×10^5
FRP-plate (thickness 1.2 mm.)		2200	1.5×10^5
Concrete	Compressive strength = 45 MPa		

of bonded length on peeling mode of FRP. Here, the authors selected two FRP-strengthened beam specimens (A-200-P and B-200-P) and one control (non-strengthened) beam (specimen A) for verification with FEM. The cross section and reinforcement arrangement of the beams are shown in Figure 8. The load set-sup and FRP installation are given in Figure 9. The material properties of this experiment are given in Table 1. In the experiment, it was found that A-200-P fails by shear-flexural peeling and B-200-P by end peeling. These failures are target of FEM verification.

Figure 10 shows the comparison between FEM and experimental results for all beams tested.

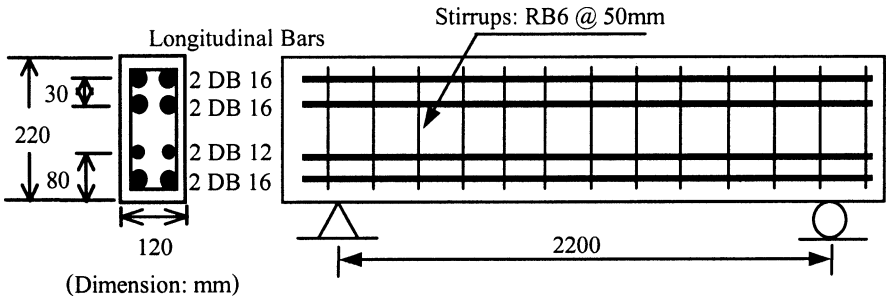

Figure 8. Cross section and reinforcement detailing.

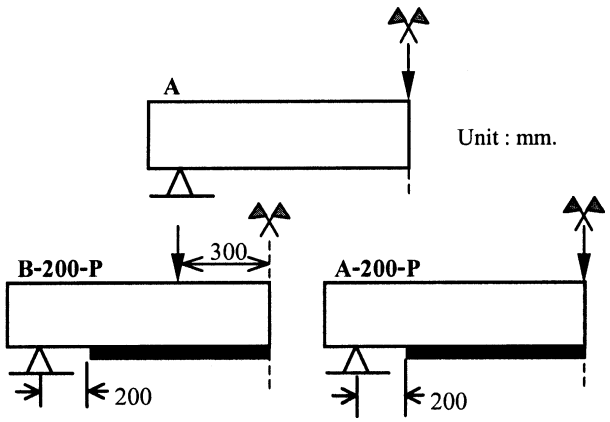

Figure 9. load method applied to the specimen.

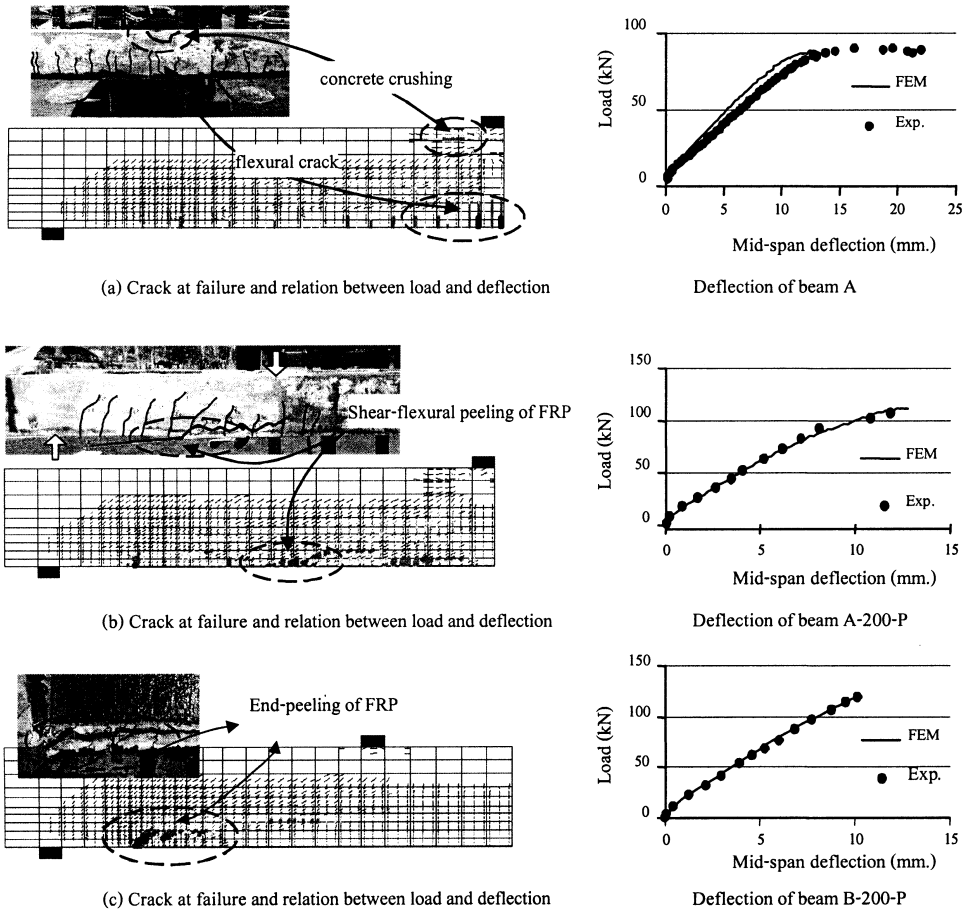

Figure 10. comparison of non linear finite element analysis and experiment for each beam.

As shown in the figure, the analytical load-displacement relations perfectly match the experimental results for all beams. As shown in Figure 10(a), in case of control beam (specimen A), the FEM predicts large flexural cracks at the bottom side of the beam near mid-span region, indicating the flexural yielding observed in the experiment. The FEM can also capture horizontal cracks near loading point, signifying concrete crushing. As for A-200-P (Figure 10(b)), FEM predicts the shear-flexural peeling indicated by concentration of diagonal cracks at the location between plate end and loading point, similar to the experiment. In case of B-200-P (Figure 10(c)), the FEM can also predict the localization of diagonal crack at the plate end similar to the experiment.

The development of cracks in A-200-P is shown in Figure 11. When the load is low (Figure 11(a)), the crack and strain distribution are similar to those of control beam. As the load increases (Figure 11(b)), a concentration of strain appears at the plate end, but does not actively propagate far enough to bring about failure. As further load is applied (Figure. 11(c), the active concentration of strain appears at a new location, which is approximately half way between plate end and loading point. This strain concentration is equivalent to the shear-flexural peeling observed in the experiment.

The development of cracks in B-200-P is shown in Figure 12. When the load is low (Figure 12(a)), the crack and strain distribution are similar

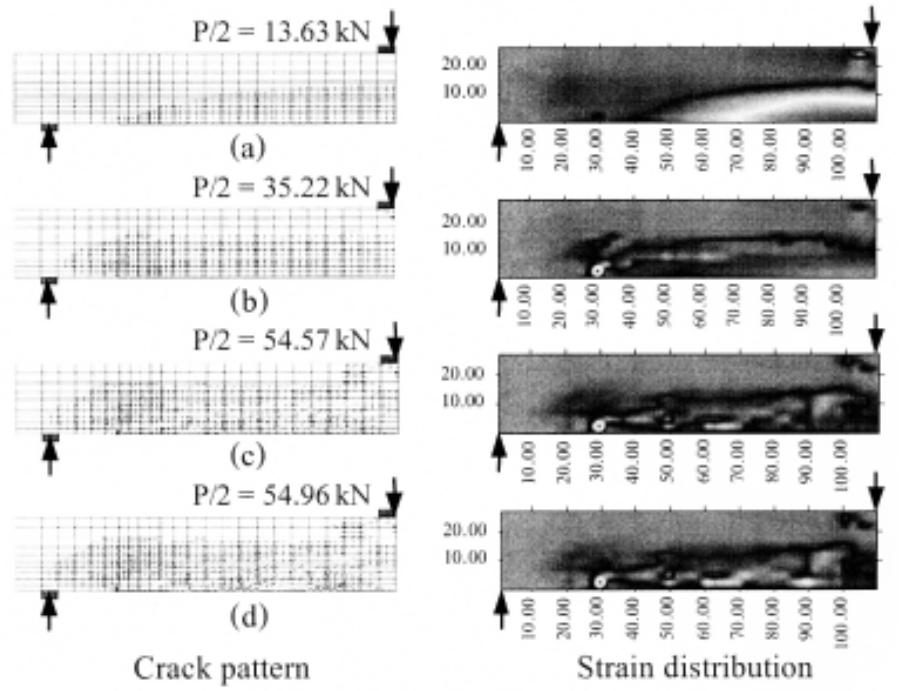

Figure 11. Development of cracks and strain corresponding to shear-flexural peeling (beam A-200-P) .

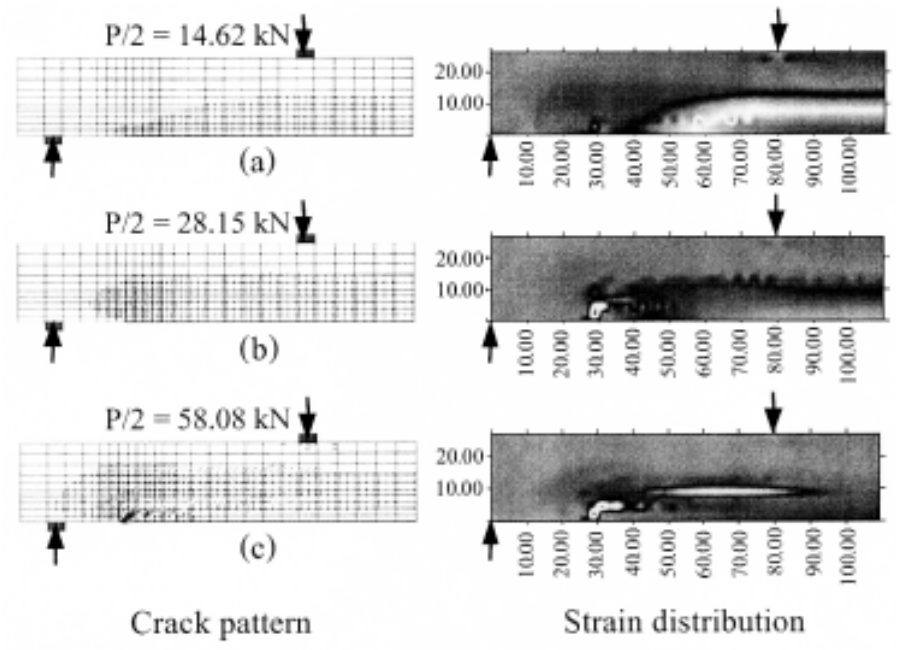

Figure 12. Development of cracks and strain corresponding to end-peeling failure (beam B-200-P).

to those of control beam. As the load increases (Figure 12(b)), a concentration of strain appears at the plate end and actively propagates into the beam, indicating the end peeling failure observed in the experiment. From these results, it is seen that FEM with nonlinear constitutive models can be used to predict the load-displacement relation, the load capacity and failure mode of FRP-strengthened beam accurately. It can also capture the local development of cracking process for both shear-flexural peeling and end peeling failure modes.

Conclusion

Finite element analysis using non-linear constitutive models of cracked concrete, steel bars and FRP is used to predict the behavior of FRP-strengthened beam. It is verified that the finite element analysis can accurately predict the load-deformation, load capacity and failure mode of the beam. It can also capture cracking process for the shear-flexural peeling and end peeling failures, similar to the experiment.

Reference

Arduini, M. and Nanni, A., 1997. Parametric Study of Beams with Externally Bonded FRP Reinforcement, ACI Struct. J., 94(5): 493-501.

Fukuura, N., Maekawa, K.,1999 Spatially averaged constitutive law for RC in-plane elements with non-orthogonal cracking as far as 4-way directions, Proc. of JSCE, Vol.45: 177-195

Hollaway, L.C., Leeming, M.B., 1999. Strengthening of reinforced concrete structures using externally-bonded FRP composites in structural and civil engineering, CRC Press Ehsani, M.R.

Maekawa, K, Pimanmas, A. and Okamura, H., 2003. Nonlinear mechanics of reinforced concrete, Spon Press, London

Okamura, H., Maekawa, K., 1991. Nonlinear analysis and constitutive models of reinforced concrete, Gihodo-Shuppan Co., Tokyo

Pornpongsaroj, P., Pimanmas, A, 2003. A. Effect of end wrapping on peeling behavior of FRP-strengthened beams. Proceedings of the Sixth International Symposium on Fibre-Reinforced Polymer Reinforcement for Concrete Structures (FRPRCS-6)., Singapore, July 8-10, Vol.1: 277-286.

Ritchie P.A., Thomas D.A., Lu L.W. and Connelly G.M., 1991. External reinforcement of concrete beams using fiber reinforced plastics, ACI Struct. J., 88(4): 490-500.

Saadatmanesh, H., Ehsani, M.R., 1990. Fiber composite plates can strengthen beams, Conc. Int., 12(3): 65-71.